Punching Verification of Edge Columns Assisted by Numerical Simulation and Field Testing

Alexander Kagermanov[1(✉)] and Julian Pernstich[2]

[1] Eastern Switzerland University of Applied Science (OST), Rapperswil, Switzerland
alexander.kagermanov@ost.ch
[2] Pernstich Ingenieure GmbH, Zürich, Switzerland

Abstract. The application of Swiss codes for existing structures (SIA 269/2) to the assessment of a 50-year-old 40 cm thick reinforced concrete slab under gravity loads resulted in insufficient punching capacity in the edge column regions. As a result, detailed nonlinear finite element analyses were undertaken on an isolated edge column using three-dimensional solid finite elements and high-fidelity constitutive models for cracked concrete. Results indicated that the critical mode of failure was flexural yielding and not punching. Sensitivity studies indicated that punching could potentially take place if the bottom tension reinforcement ratio at mid-span was higher. For further verification of the numerical model and structural safety of the slab, in-situ load testing was performed with the aid of flexible water tanks placed around the edge column targeting a uniform load of 5 kN/m^2. Based on detailed nonlinear finite element simulations combined with in-situ load testing with deflection and crack pattern control, it was possible to satisfy serviceability and ultimate limit states of the slab and omit lengthy and costly structural retrofitting measures.

Keywords: edge column · field testing · finite element · nonlinear analysis · punching · reinforced concrete

1 Introduction

An increasing number of existing structures require assessment due to changes in configuration, increased loads or material ageing. In order to achieve economical and environmentally sustainable solutions advanced methods of analysis capable of making reliable predictions are required. These methods offer a deeper understanding when combined with simplified models and allow verifying common engineering assumptions used in design of new structures and which not always succeed in identifying critical load paths and governing failure mechanism.

The current paper presents an example were both engineering methods and advanced nonlinear finite element analyses (NLFEA) were used to verify an existing 50-year-old concrete slab. Detailed NLFEA was undertaken to check the punching capacity of edge columns, which was deemed insufficient according to the Swiss Code for existing structures (SIA 269/2) [1]. For further verification of the numerical model and structural

A. Ilki et al. (Eds.): *fib* Symposium 2023, LNCE 350, pp. 90–98, 2023.
https://doi.org/10.1007/978-3-031-32511-3_10

safety of the slab, in-situ load testing was performed with water tanks placed around the edge column. Based on simulation results combined with in-situ load testing, it was possible to avoid lengthy and costly structural retrofitting measures.

2 Description of the Existing Structure

The investigated slab is part of a shopping mall built in 1972 in the Kanton of Tessin (Switzerland). Given the large dimensions of the floor area (approximately 12000 m^2), thermal joints were introduced subdividing the slab into eight sections. Such a section is shown in (Fig. 1). It consists of a 40 cm-thick reinforced concrete (RC) slab supported on RC columns and an edge wall on the north side. The spans between columns are 8.65 m and 10 m in the x and y directions, respectively. Interior columns present an hexagonal cross-section which is increased at the top creating an hexagonal capital to alleviate punching stresses. Edge and corner columns located along the joints are split in half and quarter column sections, respectively (Fig. 1).

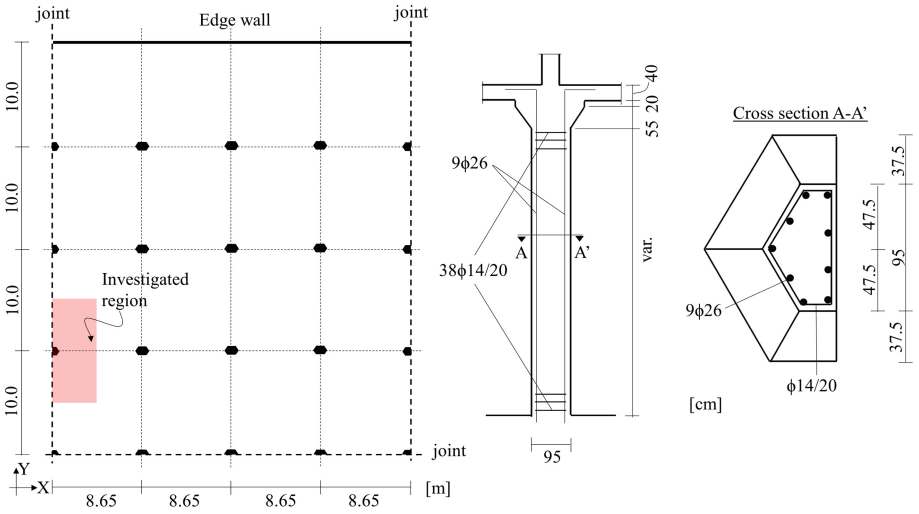

Fig. 1. Plan view of an existing slab section, typical edge column elevation and cross-section.

Existing drawings showed very low amount of top longitudinal reinforcement in the edge column region perpendicular to the edge (reinforcement ratio $\rho_x = 0.16\%$), which was four times less compared to interior connections. This low amount of reinforcement triggered concerns on the bending and punching capacity of edge connections for an increased design live load of 5 kN/m^2.

Site investigations corroborated the presence of low reinforcement ratios in the edge regions. Field tests on concrete cores extracted from the slab showed high values of compressive strength of about 60 N/mm^2. The reinforcement steel was classified as type IIIa, with a characteristic yield strength of 450 N/mm^2. Overall, the structure was in a good durability state. No concerning signs of corrosion and cracking were identified.

3 Punching Verification According to Design Code

According to SIA 269/2 "Maintenance of Structures – Concrete" Sect. 4.3.2, punching assessment of existing slabs without punching reinforcement is performed with the same resisting model as that for new structures, which is presented in SIA 262 "Concrete Structures" [2]. The only additional comment concerns the use nonlinear analysis for the calculation of the load-slab rotation curve, which states that, for punching verification, the maximum slab rotation at a distance 2d (d = average flexural depth of the slab) from the critical section should be used.

The SIA262 design equations for checking the punching capacity of flat-slab structures without punching reinforcement are summarized in Table 1. The resisting model is based on the Critical Shear Crack Theory (CSCT) [3], which uses a slab rotation dependent failure criterion. The punching capacity is thus found at the intersection between the capacity and the load-slab rotation curve.

Table 1. Summary of punching design equations according to SIA262.

Description	Equation	Number
Punching capacity (V_{Rdc})	$V_{Rdc} = k_r \tau_{cd} d_v u$	(1)
	$k_r = 1/(0.45+0.18\psi d k_g) \leq 2$	(2)
	$k_g = 48/(16+D_{max})$	(3)
	$\tau cd = 0.3\eta_t (f_{ck})^{1/2}/\gamma_c$	
	ψ: slab rotation; D_{max} maximum aggregate size; η_t: takes into account load duration; f_{ck}: characteristic value of the concrete compressive strength; γ_c: material safety factor.	(4)
Load-slab rotation	$\psi = 1.5(r_s/d)(f_{sd}/E_s)(m_{sd}/m_{Rd})^{3/2}$	
	r_s: distance between column axis and point of zero moment; f_{sd}: yield strength of steel; E_s: elastic modulus; m_{sd}/m_{Rd}: ratio between applied and resisting moments	(5)

According to SIA262, Eq. (5) can be applied with different levels of approximation. If the ratio between spans satisfies $0.5 \leq l_x/l_y \leq 2$ and no significant redistribution of plastic moments is expected, then $r_s \approx 0{,}22 l_x$ and $m_{sd}/m_{Rd} \approx 1$ (Level I). If $0.5 \leq l_x/l_y \leq 2$ and plastic redistribution is expected, simplified formulas for the estimation of m_{sd} are provided (Level II). For the rest of cases, r_s and m_{sd} can be estimated from linear static analysis (Level III).

Equation (5) was originally derived for interior axisymmetric slabs in [3], assuming that the flexural strength is reached for a radius of the yielded zone equal to $0.75 r_s$. For non-axisymmetric cases, i.e. unequal spans, moments or reinforcement ratios, punching should be checked in the direction of maximum slab-rotation. For eccentric connections with unbalanced moment, such as edge columns, a reduction factor on the perimeter is introduced. This is given as:

$$k_e = 1/(1 + e_u/b) \tag{6}$$

where e_u is the eccentricity between the resultant of the reaction and the centroid of the critical section and b the diameter of an equivalent circle with the same are as the critical section. For edge columns $k_e \approx 0.7$.

In the present case, the m_{sd}/m_{Rd} ratio perpendicular to the edge is greater than one and therefore Level I cannot be applied. If considering plastic redistribution and using simplified code formulas for m_{sd}, $\psi_x = 0.056$ rad (Level II). In this later case, the corresponding punching capacity is $V_{Rd} = 378$ kN, which is significantly lower than the design load of $V_d = 1080$ kN. Given that the punching capacity is not satisfied, further investigations using detailed FE analysis were undertaken.

4 Nonlinear FE Analysis

4.1 3D Constitutive Model for Concrete

The nonlinear material model for concrete was a smeared-crack fixed-crack orthotropic model previously verified for reinforced concrete members [4–6] (Fig. 2). In these type of models, equivalent constitutive laws in tension, compression and shear are applied in the crack directions. The compressive strength may be reduced due to orthogonal tensile strains (compression softening) or increased due to multi-axial confinement. In tension, fracture energy and mesh objectivity considerations are introduced. Shear stresses and strains arising on the crack are related through a shear retention factor, which is assumed constant after cracking. The maximum shear that can be transferred across cracks is limited by the aggregate interlock resistance [7].

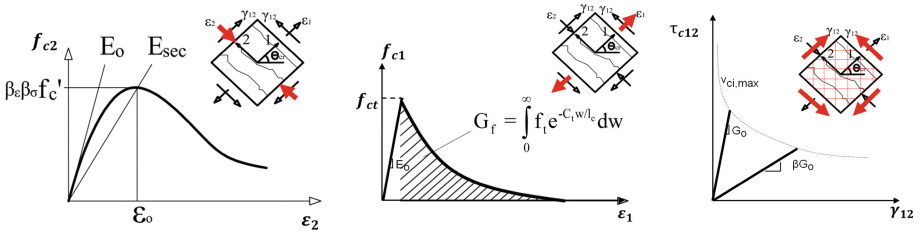

Fig. 2. Summary of constitutive models for cracked concrete in compression, tension and shear.

4.2 Validations with Existing Punching Tests

A number of punching tests were modelled in order to validate the numerical strategy. Figure 3 compares experimental and numerical results for interior column connections tested in [8] under gravity loads. All specimens experienced punching failure. Specimens PG1 and PG4 were full-scale specimens of dimensions 3000 mm × 3000 mm × 250 mm, with the main difference being the reinforcement ratio of 1.5% and 0.25%, respectively. Consequently, specimen PG1 failed in brittle punching, whereas PG4 experienced extensive yielding of longitudinal top reinforcement. Specimen PG3 was a double-size specimen of dimensions 6000 mm × 6000 mm × 500 mm. The numerical model overestimated crack-initiation for this specimen, however good agreement was shown in terms of failure load and slab rotation capacity.

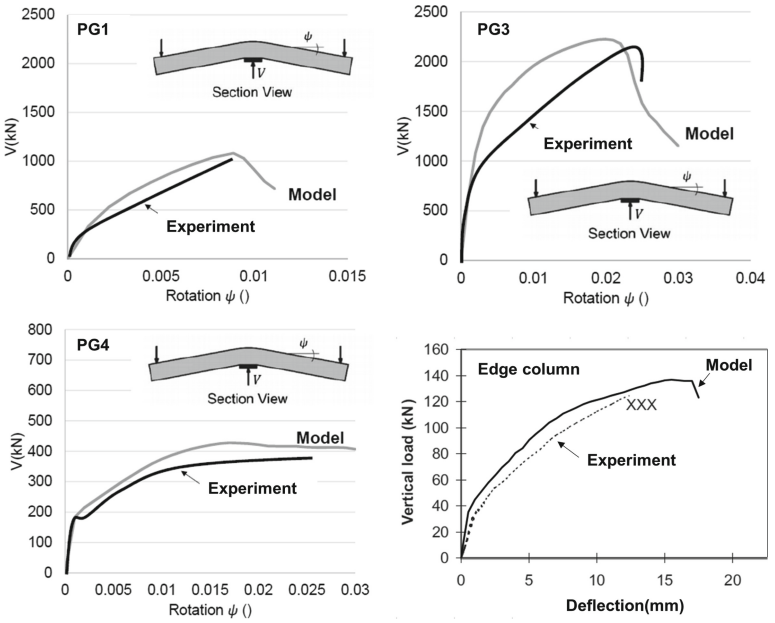

Fig. 3. Verification studies of the numerical model performed on interior and edge columns.

Additional validation studies on edge-column connections were also conducted. The specimen XXX tested in [9] featured an edge column of cross-Section 250 mm × 250 mm connected to a 120 mm-thick RC slab with typical flexural reinforcement according to design standards. Horizontal and vertical forces were applied at column ends, creating an unbalanced moment and shear with an eccentricity of e = M/V = 0.3 m. Ultimately failure occurred due to brittle punching. The numerical model showed good agreement with the experiment.

4.3 Verification of the Existing Edge Column

A detailed FE model of the existing edge column presented in Sect. 2 was created using the FE Software XDEEA [10]. 8-node solid elements were used to model a portion of the slab and the top and bottom columns (Fig. 4). The bottom column was fully restrained at the base. The horizontal displacement of the top column was restrained. Symmetric boundary conditions were assumed for the slab interior edges.

The slab was subdivided into different groups of elements for the definition of longitudinal reinforcement, which was smeared within top and bottom elements. Reinforcement ratios were reduced in the regions where insufficient anchorage was observed. Steel was modeled with a uniaxial elasto-plastic stress-strain model with strain hardening. A summary of material properties used in the numerical simulation are presented in Table 2.

Table 2. Summary of material properties used in the numerical simulation.

Concrete		Steel	
Mean compressive strength, f_{cm}	57.5 N/mm^2	Mean yield strength, f_{ym}	57.5 N/mm^2
Mean tensile strength, f_{tm}	2.5 N/mm^2	Mean tensile strength, f_{um}	2.5 N/mm^2
Tangent Modulus, E_c	38000 N/mm^2	Young Modulus, E_s	200000 N/mm^2
Peak strain at ε_{co}	0.002	Fracture strain, ε_{su}	0.10
Fracture Energy, G_f	40 N/m	Strain hardening ratio, b	0.005

A constant axial load was defined at the top of the column. A uniform incremental load was defined over the slab, which was increased until failure. The analysis used a displacement-control procedure in order to trace the post-peak behavior. The vertical displacement at the corner of the slab was chosen as controlling degree of freedom.

The load – displacement response using mean values of material strengths is shown in Fig. 4. The following sequence of failure mechanisms was identified: (1) slab cracking initiation around edge column, (2) yielding of top x-reinforcement, (3) slab bottom cracking at mid span, (4) concrete crushing in the column capital, (5) yielding of bottom reinforcement at mid span. It can be said that, overall, the slab developed a ductile flexural failure. Punching failure did not occur. Crack patterns, deformed shape and steel stresses are shown in Fig. 5 and Fig. 6.

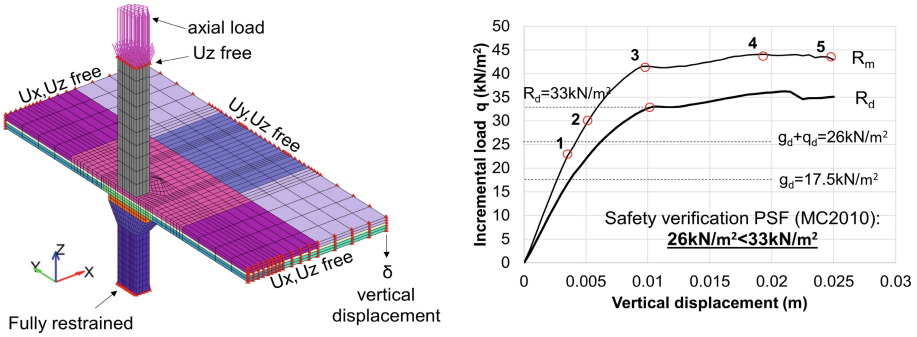

Fig. 4. FE model of a portion of the existing slab (left) and load-displacement response using mean and design values of material strengths (right).

Safety verification was performed using the Partial Safety Factor method (PSF) [11], using design values of material strengths (Fig. 4). The type of failure mechanisms remained unchanged despite the introduction of safety factors. The design capacity was estimated as 33 kN/m^2, which is greater than the applied design load of 26 kN/m^2.

Additional analyses were performed in order to investigate the likelihood of punching failure. It was seen that punching failure could occur if, for example, the amount of bottom tension reinforcement at mid span was higher. This stiffens the response after cracking

and delays the formation of a yield line at mid span. As a result, the axial load in the edge column and associated punching shear stresses continue to increase despite yielding of top tension reinforcement in the hogging region. Figure 5 compares this situation with the original one in terms of load-slab rotation response. The slab rotation was estimated here for comparison with the CSCT as the difference between vertical displacements divided by the distance and neglecting the column rotation. Punching failure occurs at a slab rotation of $\psi \approx 0.002$ rad. This result is somewhat more conservative than the failure criterion given by the CSCT.

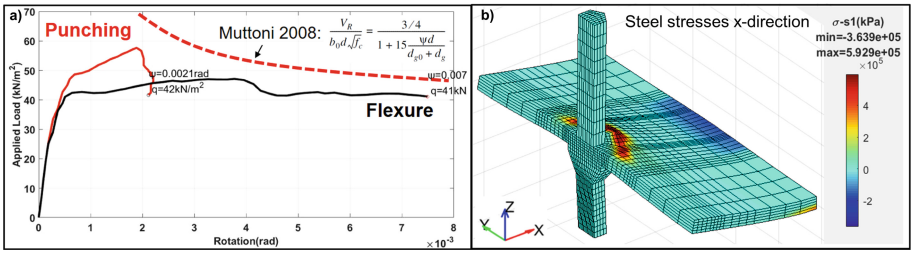

Fig. 5. (a) Comparison of load-slab rotation responses for flexural and punching failures, (b) streel stresses in the x-reinforcement in the as-build column.

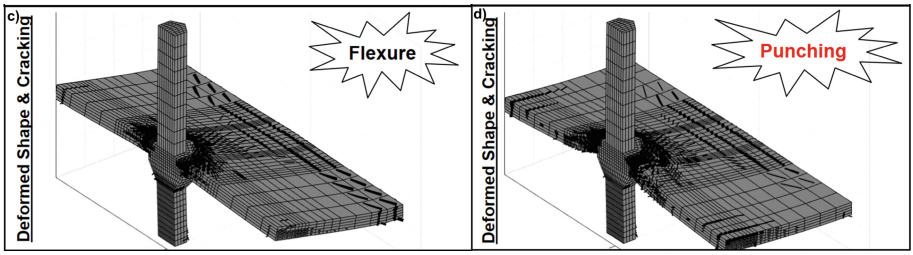

Fig. 6. Deformed shape and cracking at flexural (c) and punching failures (d).

5 Field Test

For further verification of the structural safety of the slab, in-situ load testing was performed using four flexible water tanks placed next to the edge column as shown in Fig. 7a. Displacement transducers with a tolerance of 1/100 mm were placed at six locations of the slab soffit where maximum deflections were expected and access was possible. Crack width measurements were taken before, half-way and after the test.

The water tanks were filled simultaneously until reaching a distributed load of 5.20 kN/m^2. Given the flexibility of the tanks, the initial contact area of 6 × 4.44 m^2 was reduced to 5.55 × 4 m^2 at peak load (Fig. 7b). The corresponding tank height was 50 cm. Displacement and load measurements were taken at increments of 5 cm.

The maximum displacement at 5.20 kN/m^2 was 0.43 mm. After that the slab unloaded elastically without signs of residual cracks and displacements. Existing minimal crack

widths, presumably due to shrinkage effects which are not captured in NLFEM, remained essentially unchanged during and after the load test. Figure 7c also compares results from the FE model in terms of applied load – displacement measured at locations T2, T4 and T5, where the maximum deflections occurred. It can be seen that the model was overall in good agreement with the measured values.

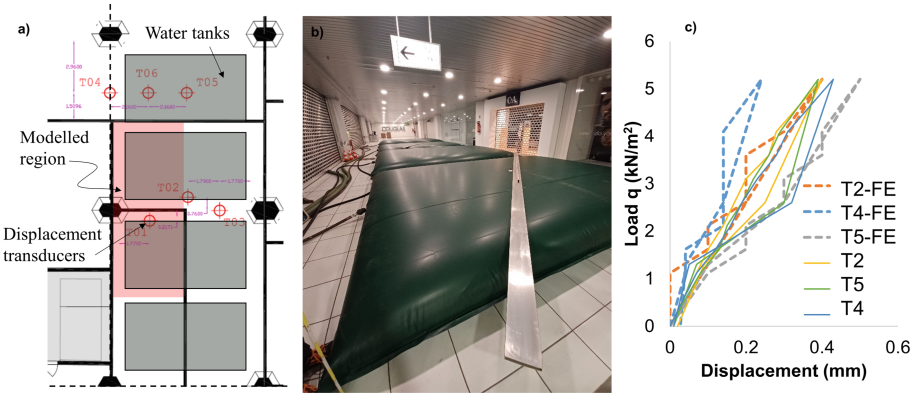

Fig. 7. (a) Loading configuration and sensor configuration of the field test, (b) water tanks at maximum capacity and (c) comparison of measured and calculated load-displacement values.

6 Conclusions

The paper highlighted some of the challenges when existing structures are verified using methods intended for design of new structures. It also showed how detailed investigations using a combination of nonlinear analysis and field-testing lead to more rational decisions by avoiding unnecessary retrofitting measures. The experimentally validated nonlinear models delivered a more realistic picture of the slab capacity and critical failure mode. The field-test allowed direct verification of the structural safety at serviceability level. The maximum applied during the test ($\approx$5 kN/m^2) corresponds to the characteristic value of live load and has, therefore, a 5% probability of being exceeded during the lifespan of the slab. Monitored deflections, stiffness and crack widths showed the excellent performance and robustness of the structure.

References

1. SIA 269 (2011) Grundlagen der Erhaltung von Tragwerken, Schweizer Norm 505 269. Schweizerischer Ingenieur- und Architektenverein, Zürich, 2013:28
2. SIA 262 (2013) Betonbau, Schweizer Norm 505 262. Schweizerischer Ingenieur- und Architektenverein, Zü-rich 102
3. Muttoni A (2008) Punching shear strength of reinforced concrete slabs without transverse reinforcement. ACI Struct J 105(4):440–450

4. Kagermanov A, Ceresa P (2016). Physically-based cyclic tensile model for RC membrane elements. J Struct Eng (ASCE) 142(12):04016118
5. Kagermanov A, Ceresa P (2018). Fiber-section model with an exact shear strain distribution for RC frame elements. J Struct Eng (ASCE) 143(10):04017132
6. Kagermanov A (2019). Finite element analysis of shear failure of reinforced and prestressed concrete beams. Hormigón y Acero, (ACHE) 70(287):75–84
7. Vecchio F, Collins M (1986) The modified compression field theory for RC elements subjected to shear. ACI J 9:82–S22
8. Guandalini S, Burdet OL, Muttoni A (2009) Punching tests of slabs with low reinforcement ratio. ACI Struct J 106(1):87–95
9. El-Salakawy EF, Pola MA, Soliman MH (1998). Slab-column edge connections subjected to high moments. Can. J. Civ. Eng. 25:526–538
10. XDEEA3D: Nonlinear FEA Software, Version 2.1 2021. https://www.xdeea.com
11. Fédération Internationale du Béton (fib): Model Code 2010 (2012) final draft, fib, Bulletin 66, Lausanne, Switzerland, 370